Charged particles in an external field: A QED analog with Bose-Einstein condensates

Shay Leizerovitch and Benni Reznik
School of Physics and Astronomy, Raymond and Beverly Sackler Faculty of Exact Sciences, Tel Aviv University, Tel Aviv 69978, Israel
(Received 21 November 2016; published 10 April 2017)

We propose a method for using ultracold atomic Bose-Einstein condensates to form an analog model of a relativistic massive field that carries charge and interacts with an external nondynamical gauge field. Such a scalar QED analog model may be useful for simulating various effects of quantum field theory involving charged particles, such as the Schwinger pair creation of charged phonons in a constant external field, and vacuum instability.

DOI: 10.1103/PhysRevA.95.043611

I. INTRODUCTION

The origins of the idea that nature manifests close analogies between phenomena at very different scales can be traced back to the dawn of science. Analogous arguments have been used, for example, to motivate the first atomistic theory of nature as beautifully described by Lucretius [1]. In contemporary physics it turns out that the idea of nature analogies is reflected more concisely in the mathematical resemblance of phenomena at very different length and time scales, from the high-energy scales of particle physics that are described by high-energy physics (HEP) to nonrelativistic atomic many-body systems and further up to the large cosmological scales and black holes in general relativity [2–4].

One research field that has particularly benefited by employing analogies has emerged from Hawking's discovery that quantum mechanical effects cause black holes to emit radiation and gradually evaporate [5,6]. In the absence of a complete theory of quantum gravity, the black-hole evaporation effect is unfortunately still only partially understood even at the fundamental level [7]. A "fluid model" of a black hole proposed by Unruh [8] provided an analog framework for studying Hawking radiation and inspired theoretical [9–14] and experimental ideas [15–24]. Remarkably, several experiments, notably with ultracold atomic condensates that mimic a black hole, provided confirmations of the Hawking effect [25–28].

While atomic condensates turned helpful in gravitational scenarios, they have been somewhat more restrictive in connection with HEP problems and so far mostly used to mimic free relativistic fields. The building blocks of the standard model of high-energy physics are gauge field theories (Abelian and non-Abelian). They are essential for understanding effects such as quark confinement in QCD. Recently, it was proposed that such models, when formulated on a lattice, can be naturally simulated using discrete setups involving ultracold atoms trapped in optical lattices [29–34].

In this article we shall suggest, however, that the analogy between atomic condensates and quantum field theory can be extended and mimic charged massive relativistic fields under the influence of an external electromagnetic gauge field. We will show that a QED analog model can be constructed using several Bose-Einstein condensates (BECs), with suitably chosen interactions.

The article proceeds as follows. In Sec. II we discuss the basic features of quantum field theory coupled to an external gauge field. We introduce the dynamical degrees of freedom of the theory, complex scalar fields, and introduce their interaction with the gauge field. In Sec. III we show, following [14] (using the Bogoliubov Hamiltonian), that a coupled two-mode condensate gives rise to a massive phonon mode that is analogous to a massive Klein-Gordon field. In Sec. IV we construct a real scalar field and its conjugate momenta using massive excitations. We then discuss the emergence of Lorentz invariance and locality. In Sec. V we further extend the condensate system and build an analog complex scalar field. We identify the charge operator, associated with global phase invariance, and identify positive and negative phonon charge carriers. In Sec. VI we construct the interaction between a charged field and an external gauge field.

II. LOCAL GAUGE INVARIANCE: SCALAR QED

We begin by briefly discussing the basic key features of quantum field theory that involve matter interacting with gauge fields. Generally speaking, we consider the simplest example of a relativistic quantum field theory for dynamical charged matter that is coupled to a gauge field, which manifests the following two fundamental key features: invariance under space-time Lorentz transformations and local gauge symmetry. As opposed to the global nature of the "external" space-time Lorentz transformations, the gauge symmetry represents the invariance of the theory under local transformation of "internal" degrees of freedom. The first property is essential to any relativistic field theory. The second property is modeled with dynamically locally conserved charge. It is well known from Noether's theorem that *local* (as opposed to global) gauge invariance gives rise to a dynamically conserved quantity, which in this case physically corresponds to a charge that is carried by the matter field.

We will consider a theory that has a U(1) gauge symmetry. Matter will be represented by a complex scalar field $\Phi(x)$ and the external gauge field by $A_\mu(x)$. Such a theory should then remain invariant under the transformations

$$\Phi(x) \to e^{i\theta(x)}\Phi(x), \quad \Phi^\dagger(x) \to e^{-i\theta(x)}\Phi^\dagger(x),$$

and

$$A_\mu(x) \to A_\mu(x) - \frac{\partial\theta(x)}{\partial x^\mu},$$

where $\theta(x)$ is an arbitrary real function.

A simple example of such a theory can be described by the Lagrangian density

$$\mathcal{L} = [D_\mu \Phi(x)]^\dagger D^\mu \Phi(x) - m^2 \Phi(x)^\dagger \Phi(x), \tag{1}$$

where $D_\mu = \partial_\mu + ieA_\mu$. It can be readily seen that indeed the theory respects both space-time and internal gauge symmetries. In particular, it gives rise to a conserved (Abelian) charge $Q = \int J_0 dx$, where $J_\mu = i(\Phi^\dagger D_\mu \Phi - \text{H.c.})$.

We will establish an analogy between the field theory described by Eq. (1) and a system involving ultracold nonrelativistic atomic condensates. Since the latter is usually described by a nonrelativistic Hamiltonian, it will be helpful to recast our quantum field theory (QFT) model in the Hamiltonian framework as well.

The corresponding Hamiltonian density $\mathcal{H}$ can be expressed in terms of the field Φ and the canonically conjugate momentum $\Pi(x)$, obeying a commutation relation $[\Phi(\mathbf{x}), \Pi(\mathbf{y})] = i\delta(\mathbf{x} - \mathbf{y})$. We have $\mathcal{H} = \mathcal{H}_0 + \mathcal{U}_E + \mathcal{U}_B$, where $\mathcal{H}_0$ is the free noninteracting part

$$\mathcal{H}_0 = \Pi^\dagger \Pi + (\nabla \Phi)^\dagger (\nabla \Phi) + m^2 \Phi^\dagger \Phi, \tag{2}$$

the term $\mathcal{U}_E$ describes the electric interaction with an external scalar field $A_0(x)$,

$$\mathcal{U}_E = ieA^0(\Pi^\dagger \Phi^\dagger - \Phi \Pi) + e^2 A_0 A^0 \Phi^\dagger \Phi, \tag{3}$$

and $\mathcal{U}_B$ is the magnetic interaction with an external vector field $\vec{A}(x)$,

$$\mathcal{U}_B = ieA^i \Phi^\dagger \overleftrightarrow{\partial}_i \Phi + e^2 A_i A^i \Phi^\dagger \Phi. \tag{4}$$

Since we consider a particular case of static external fields, the terms referred to above as scalar and vector interactions indeed correspond to electric and magnetic interactions. Furthermore, Eqs. (3) and (4) have simple physical meanings. The first term on the right-hand side of (3) (which henceforth will be denoted by $\mathcal{U}_E^{(1)}$) describes the interaction of the charged field with the electric potential $A^0 J_0$, where

$$J_0 = ie[\Pi^\dagger(x)\Phi^\dagger(x) - \Pi(x)\Phi(x)]. \tag{5}$$

The second term on the right-hand side of (3) (henceforth denoted by $\mathcal{U}_E^{(2)}$) is quadratic in A^0. In strong electric fields, it gives rise to quantum relativistic effects such as pair creation and instability of the vacuum. The first term on the right-hand side of (4) (henceforth denoted by $\mathcal{U}_B^{(1)}$) is the well known $\vec{A} \cdot \vec{J}$ interaction. Finally, the last term, proportional to $\vec{A}^2$ (henceforth denoted by $\mathcal{U}_B^{(2)}$), becomes important at strong magnetic fields. For example, in the nonrelativistic case, it produces the Landau energy-level structure in two-dimensional electronic systems.

In the following, it will be useful to recast the above Hamiltonian in terms of real scalar fields. It can be readily seen that the free Hamiltonian part (2) can be reexpressed in terms of two scalar fields ϕ_i $i = 1,2$ and their conjugate momenta. The fields are given by the real and imaginary parts of the original complex field $\phi_1 = \sqrt{2}\,\text{Re}\Phi$ and $\phi_2 = \sqrt{2}\,\text{Im}\Phi$, respectively. Similarly, their conjugate fields are obtained from $\Pi(x)$. The free Hamiltonian in this representation is then given by the linear combination $\mathcal{H}_0 = \mathcal{H}_0(\phi_1,\pi_1) + \mathcal{H}_0(\phi_2,\pi_2)$. We should notice, however, that in this bifield representation, the electric and magnetic interactions (3) and (4) contain quadratic mixed terms proportional to $\phi_i \phi_j$.

III. MASSIVE PHONONS IN A BEC

The Bogoliubov spectrum of phonon excitations in a BEC is linear at small momenta and hence analogous to a single massless scalar field. An elegant method that gives rise to a spectrum of massive relativistic particles, that is, to "massive phonons" in a BEC, has been suggested [14]. The scheme starts with a two-mode condensate system and introduces a Raman coupling between the condensates. The resulting normal modes of the uncoupled condensates are deformed by the coupling; one of the two dispersion branches remains massless and the second acquires effective mass. In the hydrodynamical approximation, the latter corresponds to a relativistic massive particle with a Klein-Gordon energy-momentum relation $E = \sqrt{m^2c^4 + c^2p^4}$.

In the following we consider a Hamiltonian density of two condensates

$$\mathcal{H} = \mathcal{H}_{\text{GP}} + \mathcal{H}_L, \tag{6}$$

where

$$\mathcal{H}_{\text{GP}} = \sum_{i,j=1}^{2} \frac{\delta_{ij}}{2m} |\nabla \psi_i(\mathbf{x})|^2 + U_{ij} |\psi_i^\dagger(\mathbf{x}) \psi_j(\mathbf{x})|^2 \tag{7}$$

and

$$\mathcal{H}_L = \Omega_M(\psi_2^\dagger(\mathbf{x})\psi_1(\mathbf{x}) + \text{H.c.}) \tag{8}$$

are the free Gross-Pitaevskii Hamiltonian density and laser- (or microwave-) induced interaction, respectively, with m the mass of the condensate atoms, U_{ij} the scattering coefficients, and Ω_M the Rabi frequency. The total Hamiltonian is $H = \int d^3\mathbf{x}\,\mathcal{H}$.

By expanding the condensates' fields ψ_i around their mean field $\bar{\psi}_i$ as $\psi_i(\mathbf{x}) = \bar{\psi}_i + \delta\psi_i(\mathbf{x})$, where $\delta\psi_i(\mathbf{x})$ are small enough perturbations, and furthermore assuming that the condensates are uniform and $\bar{\psi}_1 = \bar{\psi}_2 = \sqrt{n}$, we can approximate H by a quadratic Hamiltonian in terms of $\delta\psi_i(\mathbf{x})$. The latter can be diagonalized by expanding

$$\delta\psi_i(\mathbf{x}) = \int d^3\mathbf{p}\, a_{i,\mathbf{p}} e^{i\mathbf{p}\cdot\mathbf{x}} \tag{9}$$

and then performing a Bogoliubov transformation (see Appendix A). For the following it will be convenient to redefine the integration on the momentum space as

$$\int d^d\mathbf{p} \equiv \int \frac{d^d\mathbf{p}}{(2\pi)^{d/2}}. \tag{10}$$

The Bogoliubov transformation leads to

$$a_{i,\mathbf{p}} = \frac{1}{\sqrt{2}} \sum_{J=(0,M)} [u_{i,J}(\mathbf{p}) b_{J,\mathbf{p}} + v_{i,J}(-\mathbf{p}) b^\dagger_{J,-\mathbf{p}}]. \tag{11}$$

The first normal mode $J = 0$ turns out gapless. The second normal mode $J = M$ is gapped with $E = Mc_s^2$ at $\mathbf{p} = 0$, as illustrated in Fig. 1.

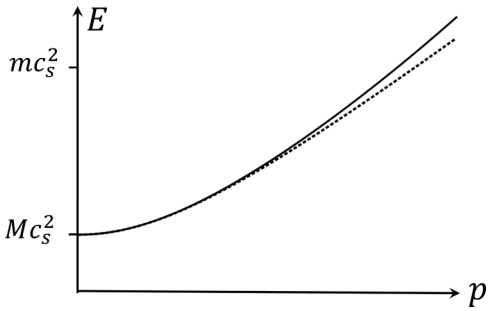

FIG. 1. Gapped dispersion relation. The dotted line denotes an ideal Klein-Gordon energy. The solid line corresponds to the mode $J = M$. Beyond the cutoff energy scale $E_{\text{cutoff}} \sim mc_s^2$, the two energies begin to deviate.

The Bogoliubov amplitudes are given by

$$u_{i,0}(\mathbf{p}), v_{i,0}(-\mathbf{p}) = \pm\sqrt{\frac{mc_{s0}^2 + \epsilon_p}{2E_0(p)} \pm \frac{1}{2}} \tag{12}$$

and

$$u_{i,M}(\mathbf{p}), v_{i,M}(-\mathbf{p}) = \pm(-1)^i\sqrt{\frac{mc_{sM}^2 + \epsilon_p}{2E_M(p)} \pm \frac{1}{2}}, \tag{13}$$

where $\epsilon_p = p^2/2m$. The complete expressions for the massless and massive dispersion branches are given in Appendix A. (They may be of much interest, for example, close to sonic black-hole horizons, which mix low and high frequencies [9–11,13,17].) For small energies, the gapped mode agrees with the dispersion relation

$$E(p) = \sqrt{M^2c_s^4 + c_s^2p^2} \tag{14}$$

of a massive relativistic particle of rest mass energy Mc_s^2,

$$\frac{M^2}{m^2} = \frac{-4\Omega_M[n(U - U') - \Omega_M]}{[n(U - U') - 2\Omega_M]^2}, \tag{15}$$

where the upper limit on the speed of (massive) sound waves $c_{sM} \equiv c_s$ is define by

$$mc_s^2 = n(U - U') - 2\Omega_M. \tag{16}$$

We observe that the effective mass is imaginary and may lead to dynamical instability of the system [35]. In order to avoid it, we set Ω_M to be negative. Since the expression for $E(p)$ above holds only below the cutoff energy scale $E(p) \ll mc_s^2$, it also follows that the rest mass M of the massive phonon is smaller than the mass m of the particles that form the condensates: $M \ll m$. If we demand that the dispersion relation remains valid in the ultrarelativistic regime $E(p) = \sqrt{c_s^2p^2 + M^2c_s^4} \approx c_sp$, we must further require $Mc_s \ll p \ll mc_s$. Using (15), we can see that this bounds the Rabi frequency of the coupling laser

$$(2mL^2)^{-1} < |\Omega_M| \lesssim \varepsilon n(U - U')/2, \tag{17}$$

where ε is the ratio of the masses M/m and L is the typical length of the system. Therefore, setting the effective mass to be one order of magnitude less than the atomic mass leads to the bound $|\Omega_M| \lesssim 0.05n(U - U')$.

Having identified the massive and massless normal modes, we return to the discussion of the spatial structure of the field operators $\delta\psi_i(\mathbf{x})$. Using Eqs. (9) and (11), we can rewrite $\delta\psi_i(\mathbf{x})$ as

$$\delta\psi_i(\mathbf{x}) = \frac{1}{\sqrt{2}}[\varphi_0(\mathbf{x}) + (-1)^i\varphi_M(\mathbf{x})], \tag{18}$$

where $\varphi_M(\mathbf{x})$ and $\varphi_0(\mathbf{x})$ are complex massive and massless condensate field operators, respectively. They satisfy the commutation relations

$$[\varphi_J(\mathbf{x}), \varphi_{J'}^\dagger(\mathbf{x}')] = \delta_{J,J'}\delta(\mathbf{x} - \mathbf{x}'). \tag{19}$$

We see that the massive spatial field is given by the relative field $\varphi_M = [\delta\psi_2(\mathbf{x}) - \delta\psi_1(\mathbf{x})]/\sqrt{2}$, while the massless field corresponds to the collective combination $\varphi_0 = [\delta\psi_1(\mathbf{x}) + \delta\psi_2(\mathbf{x})]/\sqrt{2}$. In the following we omit the index J and use $\varphi(\mathbf{x})$ to denote a massive field.

The complex field $\varphi(\mathbf{x})$ can now be used to construct a single massive scalar field $\phi(\mathbf{x})$ and a corresponding conjugate momentum $\pi(\mathbf{x})$ as follows:

$$\phi(\mathbf{x}) = \frac{i}{\sqrt{2}}[\varphi(\mathbf{x}) - \varphi^\dagger(\mathbf{x})], \tag{20}$$

$$\pi(\mathbf{x}) = \frac{1}{\sqrt{2}}[\varphi(\mathbf{x}) + \varphi^\dagger(\mathbf{x})]. \tag{21}$$

Equations (20) and (21) satisfy the canonical commutation relation

$$[\phi(\mathbf{x}), \pi(\mathbf{x}')] = i\delta(\mathbf{x} - \mathbf{x}'). \tag{22}$$

The above conjugate real fields can be expressed in terms of the Bogoliubov modes as

$$\phi(\mathbf{x}) = \frac{i}{\sqrt{2}}\int d\mathbf{p}[u(\mathbf{p}) - v(\mathbf{p})](\hat{b}_\mathbf{p}e^{i\mathbf{p}\cdot\mathbf{x}} - \hat{b}_\mathbf{p}^\dagger e^{-i\mathbf{p}\cdot\mathbf{x}}), \tag{23}$$

$$\pi(\mathbf{x}) = \frac{1}{\sqrt{2}}\int d\mathbf{p}[u(\mathbf{p}) + v(\mathbf{p})](\hat{b}_\mathbf{p}e^{i\mathbf{p}\cdot\mathbf{x}} + \hat{b}_\mathbf{p}^\dagger e^{-i\mathbf{p}\cdot\mathbf{x}}). \tag{24}$$

When considering the relevant regime $E(\mathbf{p}) \ll E_{\text{cutoff}} = mc_s^2$, we can use the relation

$$[u(\mathbf{p}) + v(\mathbf{p})]^2 = [u(\mathbf{p}) - v(\mathbf{p})]^{-2} \approx \frac{E(p)}{mc_s^2} \tag{25}$$

and readily obtain

$$\phi(\mathbf{x}) = \frac{i}{\sqrt{2}}\int d\mathbf{p}\sqrt{\frac{mc_s^2}{E(p)}}(\hat{b}_\mathbf{p}e^{i\mathbf{p}\cdot\mathbf{x}} - \hat{b}_\mathbf{p}^\dagger e^{-i\mathbf{p}\cdot\mathbf{x}}), \tag{26}$$

$$\pi(\mathbf{x}) = \frac{1}{\sqrt{2}}\int d\mathbf{p}\sqrt{\frac{E(p)}{mc_s^2}}(\hat{b}_\mathbf{p}e^{i\mathbf{p}\cdot\mathbf{x}} + \hat{b}_\mathbf{p}^\dagger e^{-i\mathbf{p}\cdot\mathbf{x}}). \tag{27}$$

This coincides with the normal mode expansion for a scalar field, up to a trivial redefinition: $\hat{b}_\mathbf{p} \to i\hat{b}_\mathbf{p}$. Since the $E(p)$ above is given by the Klein-Gordon dispersion relation, it is straightforward to verify that the fields satisfy the Klein-Gordon equation.

IV. EMERGENCE OF LORENTZ INVARIANCE

Although previous sections show that the Klein-Gordon Hamiltonian is obtained in the low-energy limit, it is constructive to derive it starting from more general assumptions. Let us consider the excitation field $\varphi(\mathbf{x})$ expansion in terms of the creation operators $\hat{b}_{\mathbf{p}}$. The scalar field and conjugate momenta satisfy

$$\frac{1}{\sqrt{2}}[\pi(\mathbf{x}) - i\phi(\mathbf{x})] = \varphi(\mathbf{x}) = \int d\mathbf{p}(u_p \hat{b}_{\mathbf{p}} e^{i\mathbf{p}\cdot\mathbf{x}} + v_p \hat{b}^{\dagger}_{\mathbf{p}} e^{-i\mathbf{p}\cdot\mathbf{x}}). \tag{28}$$

We invert this equation and express the creation operators $\hat{b}^{\dagger}_{\mathbf{p}}$ in terms of the field and its conjugate momentum. Then, by substituting in the Hamiltonian $H = \int d\mathbf{p}\, E(p)\hat{b}^{\dagger}_{\mathbf{p}}\hat{b}_{\mathbf{p}}$, we obtain

$$H = \frac{1}{2}\int d\mathbf{p}\, E(p) \int d\mathbf{x}\, d\mathbf{y}\, e^{i\mathbf{p}\cdot(\mathbf{x}-\mathbf{y})}[(u-v)^2\pi(\mathbf{x})\pi(\mathbf{y}) + (u+v)^2\phi(\mathbf{x})\phi(\mathbf{y})]. \tag{29}$$

Due to the dependence of the latter on the momentum, the resulting Hamiltonian has a nonlocal structure. It does not correspond to a local and Lorentz invariant QFT. However, when considering the low-energy limit (25), the Hamiltonian reduces to

$$H \approx \frac{1}{2}\int d\mathbf{p} \int d\mathbf{x}\, d\mathbf{y}\, e^{i\mathbf{p}\cdot(\mathbf{x}-\mathbf{y})}[\pi(\mathbf{x})\pi(\mathbf{y}) + E^2(p)\phi(\mathbf{x})\phi(\mathbf{y})] = \frac{1}{2}\int d\mathbf{x}\big[\pi^2(\mathbf{x}) + c_s^2|\nabla\phi(\mathbf{x})|^2 + M^2c_s^4\phi^2(\mathbf{x})\big]. \tag{30}$$

Here we have redefined $\phi(\mathbf{x}) \equiv \phi(\mathbf{x})/\sqrt{mc^2}$ and $\pi(\mathbf{x}) \equiv \sqrt{mc^2}\pi(\mathbf{x})$ to emphasize the resemblance between the latter Hamiltonian and the one of a free scalar field. From Eq. (30) we conclude that locality and Lorentz invariance both emerge in the low-energy limit. The effective low-energy theory corresponds, as expected, to a massive free QFT.

V. "CHARGED" EXCITATIONS

Charged particles can be described by a single complex field that satisfies the Klein-Gordon equation. Alternatively, we can represent the charged field in terms of a pair of massive real scalar fields of the same mass. In the case of a free charged field, the fields remain decoupled and hence can be easily constructed using the method described in Sec. III.

We will therefore consider a four-level condensate ψ_i with $i = 1,\ldots,4$. The Raman interaction term (8) involves two pairs of (laser) coupled condensates: $\mathcal{H}_L = [\psi_2^{\dagger}(\mathbf{x})\psi_1(\mathbf{x}) + \psi_4^{\dagger}(\mathbf{x})\psi_3(\mathbf{x}) + \text{H.c.}]$. Clearly, the relative complex fields $\delta\psi_{2k} - \delta\psi_{2k-1}, k = (1,2)$, correspond to two massive complex condensate field operators, and following the same construction as in Eqs. (20) and (21), we obtain a pair of real massive scalar fields that satisfies the commutation relations

$$[\phi_i(\mathbf{x}),\pi_j(\mathbf{x}')] = i\delta_{ij}\delta(\mathbf{x}-\mathbf{x}'), \tag{31}$$

with $i,j = (1,2)$.

Finally, we can build out of the latter a single complex field $\Phi(\mathbf{x})$ and conjugate momentum $\Pi(\mathbf{x})$ as

$$\Phi(\mathbf{x}) = \frac{\phi_1(\mathbf{x}) + i\phi_2(\mathbf{x})}{\sqrt{2}}, \tag{32}$$

$$\Pi(\mathbf{x}) = \frac{\pi_1(\mathbf{x}) - i\pi_2(\mathbf{x})}{\sqrt{2}} \tag{33}$$

such that

$$[\Phi(\mathbf{x}),\Pi(\mathbf{x}')] = i\delta(\mathbf{x}-\mathbf{x}'). \tag{34}$$

The complex field can be decomposed in terms of orthogonal field operators $\hat{c}_p$ and $\hat{d}_p$ as

$$\Phi(\mathbf{x}) = \int d\mathbf{p}\sqrt{\frac{mc_s^2}{2E}}(\hat{c}_{\mathbf{p}}e^{i\mathbf{p}\cdot\mathbf{x}} - \hat{d}^{\dagger}_{\mathbf{p}}e^{-i\mathbf{p}\cdot\mathbf{x}}), \tag{35}$$

where

$$[\hat{c}_{\mathbf{p}},\hat{c}^{\dagger}_{\mathbf{p}'}] = [\hat{d}_{\mathbf{p}},\hat{d}^{\dagger}_{\mathbf{p}'}] = \delta_{\mathbf{p},\mathbf{p}'}. \tag{36}$$

Comparing Eqs. (31), (26), and (27), we find that in terms of condensate excitations, the charged excitations are created by

$$\hat{c}_{\mathbf{p}} = \frac{1}{\sqrt{2}}(i\hat{b}_{1,\mathbf{p}} - \hat{b}_{2,\mathbf{p}}),$$
$$\hat{d}_{\mathbf{p}} = \frac{1}{\sqrt{2}}(-i\hat{b}_{1,\mathbf{p}} - \hat{b}_{2,\mathbf{p}}). \tag{37}$$

So far, our system is invariant only under global U(1) (phase) transformations. In the following sections, once the external gauge field will be included, the U(1) symmetry will become local and through Noether's theorem the charge will be guaranteed to be locally conserved. We can however identify already the operator that corresponds to the global charge

$$\mathcal{Q} = ie\int d\mathbf{x}[\Pi^{\dagger}(\mathbf{x})\Phi^{\dagger}(\mathbf{x}) - \Phi(\mathbf{x})\Pi(\mathbf{x})], \tag{38}$$

where e, the unit charge, has no physical significance in the absence of interaction. Substitution of the complex field and its conjugate momentum in terms of $\hat{c}_{\mathbf{p}}$ and $\hat{d}_{\mathbf{p}}$ yields

$$\mathcal{Q} = e\int d\mathbf{p}(\hat{c}^{\dagger}_{\mathbf{p}}\hat{c}_{\mathbf{p}} - \hat{d}^{\dagger}_{\mathbf{p}}\hat{d}_{\mathbf{p}}). \tag{39}$$

We observe that excitations of type c and type d carry opposite "charges": Type c carries positive charge and type d carries negative charge. They can be regarded as antiparticles of each other. In terms of the condensates' degrees of freedom this gives

$$\mathcal{Q} = ie\int d\mathbf{p}(\hat{b}^{\dagger}_{1,\mathbf{p}}\hat{b}_{2,\mathbf{p}} - \hat{b}^{\dagger}_{2,\mathbf{p}}\hat{b}_{1,\mathbf{p}}). \tag{40}$$

Charge conservation can be seen here as due to the commutativity of the latter with the number operator and thus with the free Hamiltonian

$$[\mathcal{Q},H] = 0. \tag{41}$$

(For a free field, it is conserved for each p separately.)

Finally, we note that, due to gauge invariance, the Hilbert space of our system can be written as the direct sum of different

(total) charge sectors

$$\mathcal{H} = \bigoplus_{Q} \mathcal{H}_Q. \tag{42}$$

Charge conservation forbids transitions between the sectors; hence charge-conserving operators must have a block-diagonal form with respect to the latter decomposition to charge sectors.

The inclusion of an external gauge field term, while promoting the symmetry to a local U(1) gauge symmetry, leaves the essential features we discussed intact. However, charge conservation gives rise to a meaningful notion of a local conservation of charge; for instance, the external gauge field may produce charge, but only pairs of opposite sign.

VI. EXTERNAL GAUGE FIELD

As we have seen, the interaction with the external gauge field involves an electric (scalar) interaction (3) and a magnetic (vector) interaction (4). We next propose methods for realizing the above interactions. The realization of the electric part is more straightforward and involves only additional laser-induced interaction coupling terms between the condensates. The magnetic term $\mathcal{U}_B^{(1)}$ involves spatial derivatives and is more challenging. We show in Sec. VI B that $\mathcal{U}_B^{(1)}$ can be obtained with the help of an ancillary system.

A. Electric interactions

The scalar potential interaction contains, to first order in the charge e, quadratic products of the field and its conjugate momentum

$$\mathcal{U}_E^{(1)} = ieA^0(\Pi^\dagger\Phi^\dagger - \Phi\Pi). \tag{43}$$

In terms of the condensates' fields this gives

$$\mathcal{U}_E^{(1)} \propto (\psi_1^\dagger\psi_3 - \psi_1^\dagger\psi_4 - \psi_2^\dagger\psi_3 + \psi_2^\dagger\psi_4) - \text{H.c.} \tag{44}$$

From Eq. (44) we see that the interaction can be realized by adding laser Raman couplings, depicted schematically in Fig. 2. We can then deduce the relation

$$\Omega_1 = 2eA^0. \tag{45}$$

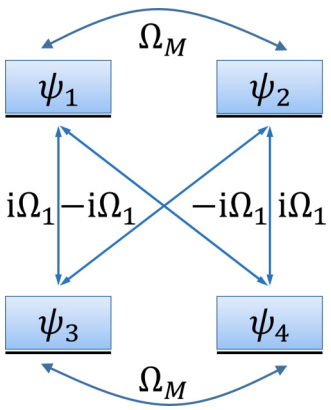

FIG. 2. Interaction of the complex field and the electric potential ($\mathcal{U}_E^{(1)}$), in terms of the analog condensates and the laser's Rabi frequency.

Moving on to consider the second-order electric interaction term, we have

$$\mathcal{U}_E^{(2)} = e^2A^0A_0\Phi^\dagger\Phi = e^2A^0A_0\frac{\phi_1^2+\phi_2^2}{2}. \tag{46}$$

This has the form of a mass term, as it is proportional to the square of the fields ϕ_i. Since the interaction does not couple the components of the complex field, one can build it separately for each field component.

To construct terms of the form ϕ_i^2, let us examine first the effect of laser-induced self-interaction of a field excitation φ_i on itself:

$$\Omega_2\varphi^\dagger\varphi = \Omega_2\frac{\pi^2+\phi^2}{2}. \tag{47}$$

Here Ω_2 is the magnitude of the effective Raman frequency of the driving laser. The interaction strength will be determined by the magnitude of the Rabi frequency Ω_2 and the magnitudes of ϕ^2 and π^2. From Eqs. (23) and (24) we see that the latter depend in turn on the amplitudes $u(\mathbf{p}) \pm v(\mathbf{p})$. Using Eq. (25), the interaction strength for an excitation with momentum p in the phonon regime can be approximated by

$$\langle\Omega_2\varphi^\dagger\varphi\rangle_p \approx |\Omega_2|\left(\frac{E}{mc_s^2}+\frac{mc_s^2}{E}\right). \tag{48}$$

Restricting the Raman frequency Ω_2 to be of the same order of magnitude as that of the phonons energy, the interaction's strength becomes

$$\langle\Omega_2\varphi^\dagger\varphi\rangle_p \approx \frac{E^2}{mc_s^2}\left(\frac{E}{mc_s^2}+\frac{mc_s^2}{E}\right) = E\left[\left(\frac{E}{mc_s^2}\right)^2+1\right]. \tag{49}$$

We observe that in the phonon regime, the first term does not contribute in the leading order and can be neglected in the three-level Hamiltonian. Namely, if the strength of the Raman frequency is on the order of the phonon's energy, then $\varphi \approx -\varphi^\dagger$.

We therefore conclude that if the Raman frequency is bounded as described above, the self-interaction term (47) gives rise to

$$2\Omega_2\varphi^\dagger\varphi \approx \Omega_2\phi^2. \tag{50}$$

Using Eq. (18), we find that the required interaction is

$$\begin{aligned}\mathcal{U}_E^{(2)} = \Omega_2(&\psi_1^\dagger\psi_1 + \psi_2^\dagger\psi_2 - \psi_2^\dagger\psi_1 - \psi_1^\dagger\psi_2 + \psi_3^\dagger\psi_3 \\ &+ \psi_4^\dagger\psi_4 - \psi_4^\dagger\psi_3 - \psi_3^\dagger\psi_4).\end{aligned} \tag{51}$$

We can now identify the relation between the Raman frequency Ω_2 and the square of the external electric potential eA^0:

$$\Omega_2 = \frac{(eA^0)^2}{mc_s^2}. \tag{52}$$

The construction of $\mathcal{U}_{\text{scalar}}^{(2)}$ in terms of the required laser couplings is depicted schematically in Fig. 3. In order to match correctly the relative strength of the electric interactions (43)

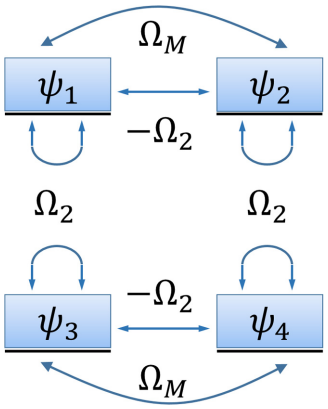

FIG. 3. Interaction of the squared gauge field and the charged scalar field ($\mathcal{U}_E^{(2)}$ or $\mathcal{U}_B^{(2)}$), given in terms of the analog condensates and the laser's Rabi frequency.

and (46), we need to tune the ratio of Ω_1 and Ω_2 such that

$$\frac{\Omega_2}{\Omega_1} = \frac{eA^0}{2mc^2}. \tag{53}$$

B. Magnetic interactions

The interaction of the charged field with the vector potential (4) contains two terms. The second-order (Landau) interaction term has a structure similar to the second-order (Schwinger) electric term (46). Therefore, it can be also realized in the same manner. We can include the second-order magnetic contribution simply by redefining Ω_2 as

$$\Omega_2 = \frac{e^2 A^\mu A_\mu}{mc_s^2}. \tag{54}$$

We note that Ω_2 also controls the strength of the vector potential interaction and thus the coupling strength of the laser that gives rise to $\mathcal{U}_B^{(1)}$ needs to be tuned as well.

The first term in Eq. (4), $\mathcal{U}_B^{(1)}$, involves spatial derivatives of the complex field. In terms of the complex field components

$$\begin{aligned}\mathcal{U}_B^{(1)} &= ieA^i \Phi^\dagger \overleftrightarrow{\nabla}_i \Phi \\ &= ieA^i(\phi_1 \overleftrightarrow{\nabla}_i \phi_1 - i2\phi_1 \overleftrightarrow{\nabla}_i \phi_2 + \phi_2 \overleftrightarrow{\nabla}_i \phi_2).\end{aligned} \tag{55}$$

To construct an interaction of this sort, we now include supplementary ancillary condensates, which will be referred to as the virtual system, and use the subscript V to denote them. The condensates that describe the physical (interacting) system will be denoted by a subscript I.

The key idea will then be to use the ancillary condensates as intermediate virtual levels and to obtain the derivative terms from second-order Raman transitions. Due to the continuous spectrum of the Bogoliubov Hamiltonian and the collective nature of its excitations, a virtual transition of atoms between the two systems may excite collective excitations in the virtual system. This can also produce undesired correlations and transfer energy between I and V.

To avoid this, we will introduce a gap in the virtual condensate by using a massive eigenmode. Therefore, our ancillary system is built of two coupled condensates. Only the massive mode of V will be coupled to the interacting system.

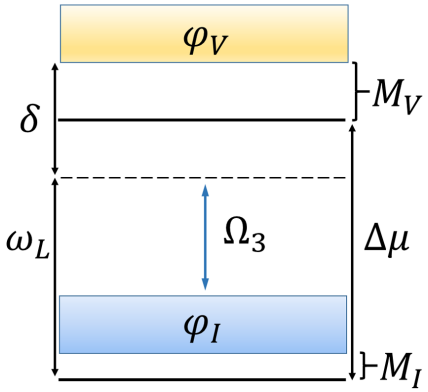

FIG. 4. Interaction between massive modes in the simulating (φ_I) and ancillary (φ_V) systems.

To avoid the undesired correlations, we set the excitations' effective mass of the virtual condensate M_V to be less than but of the order of m_I. Assuming that the excitations φ_I are in the long-wavelength regime ($p_I \ll m_I c_{sI}$), their energy scale is then much smaller than the one of φ_{M_V}. As a result, transitions of atoms between the virtual and interacting systems cannot produce excitations in the ancillary system due to energy conservation. Furthermore, we wish to prevent excitations in the interacting system due to transitions from the virtual one. In order to do so, we should reduce the temperature of the virtual system below the effective rest energy of the massive excitations, i.e.,

$$k_B T \ll M_V c_{sV}^2. \tag{56}$$

These energy constraints produce an additional energy gap between the interacting and virtual subsystems (as depicted in Fig. 4), where the difference in the two speeds of sounds yields a gap between the two chemical potentials.

Let us now construct a self-interaction of a massive excitation that contains a first-order derivative. Having discussed the properties of the ancillary system V, let us proceed to study the effect of (virtual) second-order transitions that arise from the laser-induced interaction between the virtual and interacting systems:

$$H_{\rm int} = \int d\mathbf{x}\, \Omega_3(\mathbf{x})[\varphi_V^\dagger(\mathbf{x})\varphi_I(\mathbf{x}) + \text{H.c.}], \tag{57}$$

depicted in Fig. 4.

Using the method of adiabatic elimination [36], we expand the interaction to second order in the small parameter Ω_3/δ^2. The resulting effective self-interaction of φ_I is then given by

$$H_{\rm int}^{(2)} = \int d\mathbf{x}\, d\mathbf{y}\, \Omega^*(\mathbf{x})\Omega(\mathbf{y})\varphi_I^\dagger(\mathbf{x})\varphi_I(\mathbf{y})\mathcal{I}(\mathbf{x}-\mathbf{y}). \tag{58}$$

Here the function $\mathcal{I}(\mathbf{x}-\mathbf{y})$ is the result of integrating out the intermediate virtual states

$$\begin{aligned}\mathcal{I}(\mathbf{x}-\mathbf{y}) &= \frac{\langle\varphi_V^\dagger(\mathbf{x})\varphi_V(\mathbf{y})\rangle}{\delta} \\ &= \int d\mathbf{p}\frac{|v(\mathbf{p})|^2}{\delta} e^{-i\mathbf{p}\cdot(\mathbf{x}-\mathbf{y})},\end{aligned} \tag{59}$$

where $\delta = \Delta\mu + \omega_{M_V} - (\omega_L + \omega_{M_I}) \equiv \Delta\mu + \omega_{M_V} - \Delta$. The function $\mathcal{I}(\mathbf{x}-\mathbf{y})$ is numerically evaluated in Appendix B.

Revising the energetic constraints on the interacting and the virtual systems yields further relations between the length scale

of the interacting and virtual systems. Since $m_I c_{sI}^2 \lesssim M_V c_{sV}^2$ and $\mathbf{x}-\mathbf{y} \sim (M_V c_{sV})^{-1}$ (as is shown in Appendix B), the interaction length scale is comparable to the healing length of the interacting condensate $\mathbf{x}-\mathbf{y} \lesssim (m_I c_{sI})^{-1}$. Thus, in terms of a new set of coordinates

$$\begin{aligned} \mathbf{x} &= \tfrac{1}{2}(\mathbf{X}_+ + \mathbf{X}_-), \\ \mathbf{y} &= \tfrac{1}{2}(\mathbf{X}_+ - \mathbf{X}_-), \end{aligned} \tag{60}$$

the effective interaction (58) can be expanded in terms of X_- around X_+. Since (58) is rotationally symmetric, this expansion contains only derivatives of even order and thus the first-order derivative terms that we seek are excluded. Nevertheless, giving the Rabi frequency a harmonic profile $\Omega_3(\mathbf{x}) \to \exp\{i\mathbf{k}\cdot\mathbf{x}\}\Omega_3(\mathbf{x})$ breaks the rotational symmetry and defines the derivative's orientation. Expanding the effective interaction to first order in X_- yields two terms. The first (proportional to X_-^0) has the form of a second-order Raman transition and thus can be compensated (see Appendix B). The second term (proportional to X_-) contains first-order derivatives oriented in the direction of $\mathbf{k}$ and is given by

$$H_{\text{eff}} = i\int dX_+ \Omega_3^2(X_+)\mathcal{G}\varphi_I^\dagger(\mathbf{X}_+)\overleftrightarrow{\nabla}_{\mathbf{k}}\varphi_I(\mathbf{X}_+), \tag{61}$$

where $\mathcal{G} = \mathcal{G}(\mathbf{k}, m, c_{s_I}, c_{s_V})$ is a real function (see Appendix B).

Substituting the massive excitation in terms of the scalar field and its conjugate momentum (20,21) in Eq. (61) leads to terms that breaks the local U(1) invariance of the theory. In order to avoid them, the effective Rabi frequency $|\Omega_3|^2\mathcal{G}$ should be bounded, following similar arguments used in the construction of (46). Assuming that the energy scale of the massive excitations is much smaller than the cutoff energy and

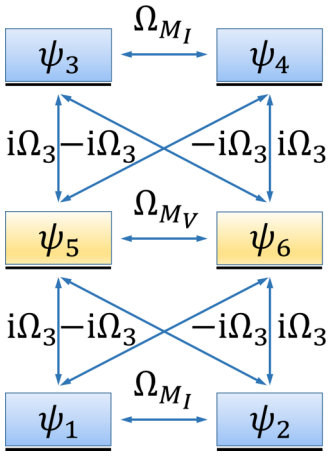

FIG. 5. Complete interaction between the simulating $\{\psi_1,\ldots,\psi_4\}$ and ancillary $\{\psi_5,\psi_6\}$ systems, given in terms of the analog condensates and the driving laser's Rabi frequency. According to (63), the coupling terms of ψ_1 and ψ_2 with the ancillary system are multiplied by a real Rabi frequency and the coupling terms of ψ_3 and ψ_4 with the ancillary system are multiplied by an imaginary Rabi frequency. This construction leads to the effective interaction, which in turn yields the interaction of the charged field with the vector potential.

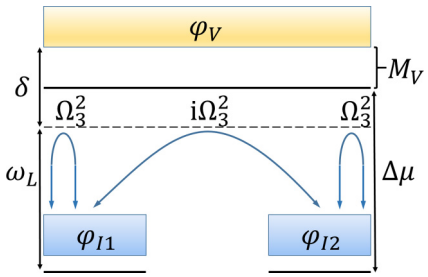

FIG. 6. Effective interaction between the modes in the interacting system.

that $|\Omega_3|^2\mathcal{G} \lesssim Mc_{sI}^2$, we obtain

$$2\varphi_I^\dagger \overleftrightarrow{\nabla}_{\mathbf{k}}\varphi_I \approx \phi \overleftrightarrow{\nabla}_{\mathbf{k}}\phi. \tag{62}$$

Finally, in order to construct the full interaction (55), we need

$$H_{\text{int}} = \int d\mathbf{x}\,\Omega_3(\mathbf{x})[\varphi_{I1}^\dagger(\mathbf{x}) + i\varphi_{I2}^\dagger(\mathbf{x})]\varphi_V(\mathbf{x}) + \text{H.c.} \tag{63}$$

In Fig. 5 we describe the required interactions between BEC components. The resulting effective interaction is schematically depicted in Fig. 6. We note that the resulting effective Rabi frequency relates to the external vector potential according to

$$eA^i = \Omega_i^{\text{eff}} \equiv \Omega_{3i}^2(\mathbf{x})\,\mathcal{G}(mc_{sV}, k_i)mc_{sI}. \tag{64}$$

VII. CONCLUSION

In this article we proposed a method for simulating a QFT system of a charged scalar field coupled to an external electromagnetic field. Unlike previously studied analogs of fields in curved space-time, which require accelerating the atomic condensate, in the present method the effect of the electromagnetic field is generated in a static condensate. The interaction here was introduced by means of external lasers that couple the internal atomic levels in a certain manner. Therefore, we expect that such a system will be more stable; there are no special requirements or special limitations on the mean-field properties. Furthermore, this provides a wider and more flexible range of applicability in controlling the various electromagnetic external fields that one may wish to apply on the charged phonons. In particular, it may enable the study of the Sauter potential and its impact on the charged field and especially on its two asymptotic limits, which yields the Klein paradox and the Schwinger effect. In addition to the scattering properties that can be experimentally measured in this sort of simulation, it may be even more intriguing to observe and study the process of pair creation and vacuum instability due to an electric field. Moreover, an electric potential of this type may also be employed as a source of particles or antiparticles for other quantum simulations that involve bulk excitations, such as gravitational analogies and QFT in curved space-time.

APPENDIX A: DIAGONALIZATION OF THE BOGOLIUBOV HAMILTONIAN FOR TWO-MODE BECS

In order to find the full dispersion relation and normal modes of a coupled two-mode BEC (6), we will derive the Bogoliubov Hamiltonian. Substitution of the mean-field expansion into the GP Hamiltonian (6) yields a Hamiltonian of the form $H_0 + H_p$, where H_0 is the ground-state energy (zero momentum) and H_p is the quadratic part that describes the excitations from the condensate. Next, in order to constrain conservation of particles number, we plug

$$N_0 = N_i - \sum_{p\neq 0} \hat{a}^\dagger_{i,p}\hat{a}_{i,p} \tag{A1}$$

into H_0, keeping only quadratic terms of the form $\hat{a}^\dagger_{i,p}\hat{a}_{i,p}$ [35]. Equivalently, we can use the operator $\hat{K} = \hat{H} - \mu\hat{N}$, where the last term acts as a Lagrange multiplier [37]. The resulting Bogoliubov Hamiltonian is

$$\begin{aligned} H_p = &\sum_{j,\mathbf{p}\neq 0}\left(\frac{p^2}{2m} + nU - \Omega\right)\hat{a}^\dagger_{j,\mathbf{p}}\hat{a}_{j,\mathbf{p}} \\ &+ \frac{1}{2}nU(\hat{a}^\dagger_{j,\mathbf{p}}\hat{a}^\dagger_{j,-\mathbf{p}} + \hat{a}_{j,\mathbf{p}}\hat{a}_{j,-\mathbf{p}}) \\ &+ nU'(\hat{a}^\dagger_{2,\mathbf{p}}\hat{a}^\dagger_{1,-\mathbf{p}} + \hat{a}_{1,\mathbf{p}}\hat{a}_{2,-\mathbf{p}}) \\ &+ (nU' + \Omega)(\hat{a}^\dagger_{2,\mathbf{p}}\hat{a}_{1,\mathbf{p}} + \hat{a}^\dagger_{1,\mathbf{p}}\hat{a}_{2,\mathbf{p}}). \end{aligned} \tag{A2}$$

Since H_p is quadratic in terms of the field operators $\hat{a}_{j,\mathbf{p}}$ and $\hat{a}^\dagger_{j,\mathbf{p}}$, it can be diagonalized by a linear transformation, leading to a new set of field operators. In order to find the appropriate transformation, we adopt the diagonalization method in [38]. We begin by introducing the vector

$$\eta^\dagger = (\hat{a}^\dagger_{1,\mathbf{p}},\hat{a}^\dagger_{2,\mathbf{p}},\hat{a}_{1,-\mathbf{p}},\hat{a}_{2,-\mathbf{p}}). \tag{A3}$$

Now H_p can be written as

$$H_p = \eta^\dagger\mathcal{H}\eta. \tag{A4}$$

We then define the transformation

$$\xi^\dagger = \eta^\dagger T, \quad \xi = T^\dagger\eta, \tag{A5}$$

where T is a 4×4 matrix and ξ is composed of the free field operators $\hat{b}_{j,\mathbf{p}}$. The bosonic commutation relation of the new field operators $\hat{b}_{i,\mathbf{p}}$ implies a constraint on the transformation matrix T, by which the inverse of T is defined. Finally, plugging the transformation (A5) into the Hamiltonian (A4) yields the eigenvalue equation

$$T^{-1}\mathcal{H}JT = \mathcal{H}_D J = \begin{pmatrix} E & 0 \\ 0 & -E \end{pmatrix}, \tag{A6}$$

where E is a 2×2 diagonal matrix of the eigenenergies E_j. The matrix $J = \mathrm{diag}\{I_N, -I_N\}$ is closely related to the symplectic matrix, which is widely used in the diagonalization process of a quadratic Hamiltonian given in canonical coordinates $\{p_n, q_n\}$.

The resulting dispersion relations of the two eigenmodes are

$$\begin{aligned} E_1^2 &= 2(nU + nU')\epsilon_p + \epsilon_p^2 \\ &= 2mc_{s1}^2\epsilon_p + \epsilon_p^2, \end{aligned} \tag{A7}$$

$$\begin{aligned} E_2^2 &= (nU - nU' - 2\Omega)^2 - (nU - nU')^2 \\ &\quad + 2(nU - nU' - 2\Omega)\epsilon_p + \epsilon_p^2 \\ &= E_{\mathbf{r}}^2 + 2mc_{s2}^2\epsilon_p + \epsilon_p^2. \end{aligned} \tag{A8}$$

As one can see, the energies differ from the well-known phonon energy of a one-component BEC. In this setup one of the modes acquires an effective mass, a momentum free term, which depends only on the coupling constants of the system. In addition, the speed of sound, which can be identified as the factor of the kinetic energy (proportional to ϵ_p), is different for every mode. Hence the massive and massless eigenmodes exhibit two different sound cones and thus have different causal structures. On the other hand, the elements of the transformation matrix T^{-1} have the generic form [35]

$$u_J(\mathbf{p}), v_J(-\mathbf{p}) \propto \pm\sqrt{\frac{mc_{sJ}^2 + \epsilon_p}{2E_J} \pm \frac{1}{2}}, \tag{A9}$$

where J refers to the two eigenmodes above.

APPENDIX B: THE EFFECTIVE INTERACTION

In order to derive Eq. (61), we begin with the evaluation of $\mathcal{I}(X_-)$. We will find an analytic function that optimally describes the behavior of $\mathcal{I}(X_-)$. Then we will use the resulting function to find $\mathcal{G}$ and obtain the effective Rabi frequency Ω_i^{eff}.

The function $\mathcal{I}(X_-)$ is given by

$$\begin{aligned} \mathcal{I}(X_-) &= \frac{\langle\varphi_V^\dagger(\mathbf{x})\varphi_V(\mathbf{y})\rangle}{\delta} \\ &= \int d\mathbf{p}\frac{|v(\mathbf{p})|^2}{\delta}e^{-i\mathbf{p}\cdot\mathbf{X}_-}, \end{aligned} \tag{B1}$$

where $\delta = \Delta\mu + \omega_{M_V} - (\omega_L + \omega_{M_I}) \equiv \Delta\mu + \omega_{M_V} - \Delta$. In order to evaluate the optimal function we will proceed as follows. First, we define the ratio of the effective and the atomic masses $\alpha = M_V/m_V$. Since the interaction is off-resonance, the detuning of the laser and the chemical potential can be determined by this ratio. Thus we are left with a controlled parameter α, which is restricted to be much smaller than one. Next we choose a function and fit it to the numerical solutions for various values of α. Then we find the dependence of the analytic function's parameters on α.

In the proceeding calculation we set $c_s = 1$ and fix the parameters as follows:

$$0.08 \leqslant \alpha \leqslant 0.12, \quad \Delta\mu - \Delta = M. \tag{B2}$$

In one dimension the function $\mathcal{I}(X_-)$ is given by

$$\begin{aligned} \mathcal{I}(X_-) &= \int_{-\infty}^{\infty} dp\, e^{ipX_-}\frac{\left(\frac{p^2}{2m} + m - E(p)\right)}{E(p)[\Delta\mu + E(p) - \Delta]} \\ &= \sqrt{2}\int_{-\infty}^{\infty} d\eta\, e^{i\eta s}\frac{1 + \eta^2 - E(\eta)}{E(\eta)[\alpha + E(\eta)]} \equiv \sqrt{2}I(s), \end{aligned} \tag{B3}$$

where $s = \sqrt{2}m_V X_-$ and

$$E(\eta) = \sqrt{\alpha^2 + 2\eta^2 + \eta^4}. \tag{B4}$$

We choose $I(s)$ to be

$$I(s) = ae^{-b|s|}, \tag{B5}$$

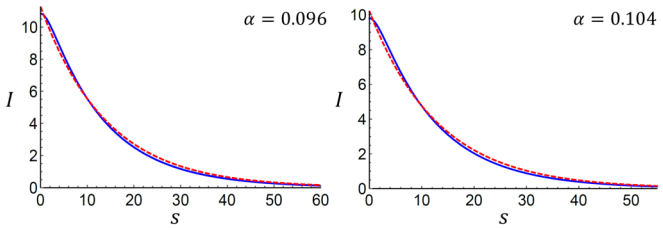

FIG. 7. Comparison between the numerical result (blue solid line) of the dimensionless integral $I(s)$ (B3) and the evaluated function (red dashed line) (B5) for different values of α in one dimension.

where a and b are both functions of α. A comparison between the numerical result and the fitted function is given in Fig. 7 for different values of α. We observe that the chosen function fits well to the numerical result and describes the general behavior of the numerical function. Next we will find the dependence of the two parameters a and b on α. In order to do so, we take the results of the two parameters for various values of α and fit a function that describes their dependence on the parameter α. The two parameters of the approximated function result in

$$a(\alpha) \approx \frac{0.64}{\alpha^{1.23}}, \tag{B6}$$

$$b(\alpha) \approx 0.56\alpha^{0.88}, \tag{B7}$$

with a comparison of the numerical results and the fitted curves given in Fig. 8. In conclusion, we obtain

$$\mathcal{I}(X_-) \approx \frac{0.9}{\alpha^{1.23}} e^{-0.8\alpha^{0.88} m_V |X_-|}. \tag{B8}$$

As one can see, the decay rate of the function $\mathcal{I}(X_-)$ is greater than M_V. Hence it dictates a characteristic length scale that is on the scale of or smaller than the interacting modes' healing length $\xi_I \equiv (\sqrt{2} m c_{sI})^{-1}$.

In two dimensions the function $\mathcal{I}(X_-)$ is given by

$$\begin{aligned}\mathcal{I}(s) &= 4\pi m_V \int_0^\infty d\eta \frac{1+\eta^2-E(\eta)}{E(\eta)[\alpha+E(\eta)]} J_0(\eta s) \\ &\equiv 4\pi m_V I(s),\end{aligned} \tag{B9}$$

where J is a Bessel function of the first kind. We repeat the procedure used in the case of the one-dimensional system and choose the evaluated function to be (B5). A comparison between the numerical results and the fitted function is depicted in Fig. 9. The two parameters of the evaluated function are given by

$$a(\alpha) = \frac{0.16}{\alpha^{0.58}}, \tag{B10}$$

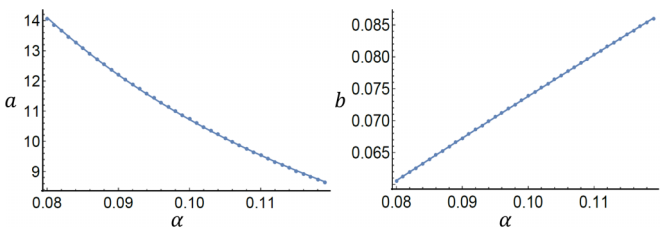

FIG. 8. Comparison between the numerical results of the parameters a and b (dots) and their evaluated functions (solid line) in one dimension, with $a(\alpha)$ and $b(\alpha)$ given in (B6) and (B7), respectively.

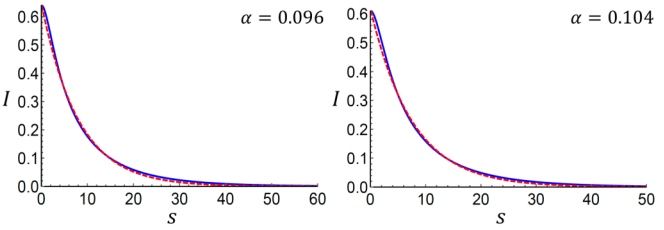

FIG. 9. Comparison between the numerical result (blue solid line) of the dimensionless integral $I(s)$ (B9) and the evaluated function (red dashed line) (B5) for different values of α in two dimensions.

$$b(\alpha) = 0.523\alpha^{0.61} \tag{B11}$$

and are plotted in Fig. 10. In conclusion, $\mathcal{I}(X_-)$ can be evaluated by

$$\mathcal{I}(X_-) \approx \frac{2m_V}{\alpha^{0.58}} e^{-0.74\alpha^{0.61} m_V X_-}. \tag{B12}$$

We observe that the evaluated function decays in the scale or faster than M_V^{-1} and hence the characteristic length scale of the interaction is in the order or smaller than the healing length of the interacting system. In conclusion, the estimation of the interaction length scale X_- is justified and the effective interaction (58) can be expanded in terms of this relatively small parameter.

We proceed with the formulation of the effective interaction (61). Expanding (58) to first order in X_- yields

$$H_{\text{eff}} = \int d\mathbf{X}_+ \Omega_3^2(X_+) \varphi_I^\dagger(\mathbf{X}_+) \hat{\mathcal{O}} \varphi_I(\mathbf{X}_+), \tag{B13}$$

where

$$\hat{\mathcal{O}} = \int dX_- \mathcal{I}(X_-) e^{i\mathbf{k}\cdot\mathbf{X}_-} (1 + \mathbf{X}_- \cdot \overleftrightarrow{\nabla}). \tag{B14}$$

Substituting (B12) into (B14), we can carry out the integration on X_-, resulting in

$$\hat{\mathcal{O}} = \mathcal{F} + i\mathcal{G} \overleftrightarrow{\nabla}_{\mathbf{k}}, \tag{B15}$$

where $\mathcal{F}$ and $\mathcal{G}$ are given by

$$\begin{aligned}\mathcal{F} &= 2m_V a \int_0^\infty dX_- X_- e^{-\sqrt{2} b m_V X_-} J_0(kX_-) \\ &= \frac{2\pi}{m_V} \frac{ab}{\left(b^2+\eta_k^2\right)^{3/2}},\end{aligned} \tag{B16}$$

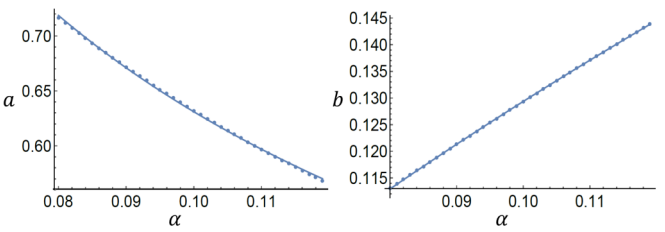

FIG. 10. Comparison between the numerical results of the parameters a and b (dots) and their evaluated functions (solid line) in two dimensions, with $a(\alpha)$ and $b(\alpha)$ given in (B10) and (B11), respectively.

$$\mathcal{G} = 2m_V b \int_0^\infty dX_- X_-^2 J_1(kX_-) e^{-\sqrt{2}bm_V X_-} = \frac{2\pi}{\sqrt{2}m_V^2} \frac{ab\eta_k}{\left(b^2+\eta_k^2\right)^{5/2}}. \quad \text{(B17)}$$

Here $\eta_k = k/\sqrt{2}m_V$ and the parameters a and b are given in (B10) and (B11), respectively. Finally, the effective interaction (58) is

$$\mathcal{H}_{\text{eff}} = \Omega_3^2(X_+)\varphi_I^\dagger(\mathbf{X}_+)[\mathcal{F} + i\mathcal{G}\overleftrightarrow{\nabla}_{\mathbf{k}}]\varphi_I(\mathbf{X}_+). \quad \text{(B18)}$$

The first term is irrelevant to our model and thus should be compensated by an additional laser-induced interaction

$$\mathcal{H}_{\text{comp}} = \Omega_{\text{comp}}[\psi_1^\dagger\psi_1 + \psi_2^\dagger\psi_2 - (\psi_1^\dagger\psi_2 + \psi_2^\dagger\psi_1)], \quad \text{(B19)}$$

where $\Omega_{\text{comp}} = -\Omega_3^2(X_+)\mathcal{F}/2$.

[1] T. Lucretius, *De Rerum Natura* (Courier Corporation, Dover, New York, 2012).
[2] F. Wilczek, Phys. Today **51**(1), 11 (1998).
[3] *Quantum Analogues: From Phase Transitions to Black Holes and Cosmology*, edited by W. G. Unruh and R. Schützhold, Lecture Notes in Physics Vol. 718 (Springer, Berlin, 2007).
[4] G. Volovik, *The Universe in a Helium Droplet* (Oxford University Press, Oxford, 2009).
[5] S. W. Hawking, Nature (London) **248**, 30 (1974).
[6] S. W. Hawking, Commun. Math. Phys. **43**, 199 (1975).
[7] S. W. Hawking, Phys. Rev. D **14**, 2460 (1976).
[8] W. G. Unruh, Phys. Rev. Lett. **46**, 1351 (1981).
[9] T. Jacobson, Phys. Rev. D **44**, 1731 (1991).
[10] T. Jacobson, Phys. Rev. D **48**, 728 (1993).
[11] W. G. Unruh, Phys. Rev. D **51**, 2827 (1995).
[12] B. Reznik, Phys. Rev. D **55**, 2152 (1997).
[13] S. Corley and T. Jacobson, Phys. Rev. D **57**, 6269 (1998).
[14] M. Visser and S. Weinfurtner, Phys. Rev. D **72**, 044020 (2005).
[15] L. J. Garay, J. R. Anglin, J. I. Cirac, and P. Zoller, Phys. Rev. Lett. **85**, 4643 (2000).
[16] L. J. Garay, J. R. Anglin, J. I. Cirac, and P. Zoller, Phys. Rev. A **63**, 023611 (2001).
[17] B. Reznik, Phys. Rev. D **62**, 044044 (2000).
[18] U. Leonhardt and P. Piwnicki, Phys. Rev. Lett. **84**, 822 (2000).
[19] P. O. Fedichev and U. R. Fischer, Phys. Rev. A **69**, 033602 (2004).
[20] T. G. Philbin, C. Kuklewicz, S. Robertson, S. Hill, F. Konig, and U. Leonhardt, Science **319**, 1367 (2008).
[21] A. Retzker, J. I. Cirac, M. B. Plenio, and B. Reznik, Phys. Rev. Lett. **101**, 110402 (2008).
[22] B. Horstmann, B. Reznik, S. Fagnocchi, and J. I. Cirac, Phys. Rev. Lett. **104**, 250403 (2010).
[23] B. Horstmann, R. Schutzhold, B. Reznik, S. Fagnocchi, and J. I. Cirac, New J. Phys. **13**, 045008 (2011).
[24] M. Elazar, V. Fleurov, and S. Bar-Ad, Phys. Rev. A **86**, 063821 (2012).
[25] O. Lahav, A. Itah, A. Blumkin, C. Gordon, S. Rinott, A. Zayats, and J. Steinhauer, Phys. Rev. Lett. **105**, 240401 (2010).
[26] S. Weinfurtner, E. W. Tedford, M. C. J. Penrice, W. G. Unruh, and G. A. Lawrence, Phys. Rev. Lett. **106**, 021302 (2011).
[27] J. Steinhauer, Nat. Phys. **10**, 864 (2014).
[28] J. Steinhauer, Phys. Rev. D **92**, 024043 (2015).
[29] E. Zohar, J. I. Cirac, and B. Reznik, Rept. Prog. Phys. **79**, 014401 (2016).
[30] J. I. Cirac, P. Maraner, and J. K. Pachos, Phys. Rev. Lett. **105**, 190403 (2010).
[31] E. Zohar and B. Reznik, Phys. Rev. Lett. **107**, 275301 (2011).
[32] U.-J. Wiese, Ann. Phys. (Leipzig) **525**, 777 (2013).
[33] N. Szpak and R. Schützhold, New J. Phys. **14**, 035001 (2012).
[34] E. Zohar, Nature (London) **534**, 480 (2016).
[35] L. Pitaevskii and S. Stringari, *Bose-Einstein Condensation* (Clarendon, Oxford, 2003).
[36] C. Cohen-Tannoudji, J. Dupont-Roc, and G. Grynberg, *Atom-Photon Interactions: Basic Processes and Applications* (Wiley, New York, 1992).
[37] C. Pethick and H. Smith, *Bose-Einstein Condensation in Dilute Gases* (Cambridge University Press, Cambridge, 2002).
[38] C. Tsallis, J. Math. Phys. **19**, 277 (1978).